Available online at www.sciencedirect.com

SciVerse ScienceDirect

Energy Procedia 14 (2012) 867 – 872

Energy Procedia

2011 2nd International Conference on Advances in Energy Engineering

# Identification of chemical composition of CRUD depositing on fuel surface of a boiling water reactor (BWR-6) plant

Tsuey-Lin Tsai[a,*], Tzung-Yi Lin[a], Te-Yen Su[a], Hwa-Jou Wei[a], Lee-Chung Men[a], Tung-Jen Wen[b]

[a]*Chemical Analysis Division, Institute of Nuclear Energy Research, Longtan, Taoyuan 32546, Taiwan, R.O.C.*
[b]*Chemistry Division, Institute of Nuclear Energy Research, Longtan, Taoyuan 32546, Taiwan, R.O.C.*

**Abstract**

The objectives of this paper aimed at the characterization of metallic composition and surface analysis on the cruds of fuel rods for unit-1 of boiling water reactor (BWR-6) at Kuosheng Nuclear Power Plant in Taiwan. The inductively coupled plasma- atomic emission spectroscopy (ICP-AES) and gamma spectrometry were carried out to analyze the corrosion product distributions and determine the elemental compositions along the fuel rod under conditions of hydrogen water chemistry (HWC) switched from normal water chemistry (NWC) of plant site in this study. Most of the crud consisted of the flakes and irregular shapes via SEM morphology. The XRD results showed that the loosely adherent oxide layer was mostly composed of hematite ($\alpha$-$Fe_2O_3$) with amorphous iron oxides. The parameters of reactor water chemistry and the available mathematical model for crud deposition were utilized to interpret the chemistry effects on such crud deposition behavior. The fuel surface of this plant appeared to be one with the lower crud deposition.



*Keywords: Hydrogen water chemistry (HWC); Normal water chemistry (NWC); Fuel cladding; Fuel rod*

## 1. Introduction

With the long-term operation of Boiling Water Reactor (BWRs), the component materials of its

* Corresponding author. Tel.: 886-3-4711400 Ext.5028; fax:886-3-4713490.
*E-mail address*: polly@iner.gov.tw.


doi:10.1016/j.egypro.2011.12.887

internal pressure boundary were easily deteriorated from intergranular stress corrosion cracking (IGSCC). The hydrogen water chemistry (HWC) injecting hydrogen from 0.5 ppm of Nov., 2006 to 1.0 ppm of Jun., 2009 was used to reduce the electrochemical corrosion potential of components, and mitigate the occurrence of IGSCC initiation and propagation in the reactor internal components and piping system [1,2]. However, the higher hydrogen concentration probably was accompanied by the adverse effect of increasing radiation levels. It is important and necessary to confirm and understand clearly the deposition behavior of corrosion products on fuel surface during such environmental change for the purpose of material integrity. Most of the radiation exposures, especially in $^{60}Co$ activity build up come from radioactive corrosion products which deposit and buildup on the inner surface of piping and components in the primary circuit are frequently observed and studied. In addition, the deposition of solid phase products on the surface of the fuel cladding in the reactor caused by corrosion products and additions to the feed water might influence the thermal and thermo hydraulic behavior of the fuel.

The crud (corrosion residual unidentified deposit) is impurities in the reactor water that deposit on hot cladding surfaces. Iron oxide is normally the primary corrosion product constituent. At high crud deposition values, crud can have a significant impact on the fuel performance. The crud deposited on fuel rods during operation can impact strongly the eddy current lift-off signal for the oxide thickness measurement, demonstrating that the deterioration results from the magnetic properties of the crud [3]. The deposition of crud varies with water chemistry, thermo hydraulic conditions in the fuel assemblies and linear heat rate of the rod position during the operation cycles and the residence time of the fuel in the core [4].

Two fuel assemblies were selected for oxide thickness measurement as well as crud analysis after almost three cycles of operation in the HWC environment, resulting in assembly average burnup of approximately 45.9 and 43.7 GWd/MTU at EOC-21 for K1D015 and K1D059, respectively [5]. Since the chemical composition and the deposited amount of crud is of interest, a measurement program with 22 crud samples of two fuel assemblies was performed at unit 1 of Kuosheng boiling water reactor (BWR) cycle in 2010. The determined amounts of crud deposit on fuel surfaces were in comparison with those calculated by available micro-layer evaporation and dry out model. The data were believed to be relatively low and Kuosheng could be considered as a low crud plant.

## 2. Experimental

XRD was employed to identify the phases of crud. The elemental and radio-isotopic compositions of the crud samples were determined in the solutions by inductively coupled plasma- atomic emission spectroscopy (ICP-AES) and gamma spectrometer.

### *2.1 Crud scraping*

Samples of crud were scraped from the fuel-cladding surface of two fuel bundles, KID015 and KID059 under water in the fuel pool using a sampling device, similar to the one sketched by Uchida and Y. Asakura [6], taken in the center of each span (Spans 1 through 5) on each of 2 sides (L5 and A5), and sucked off by a water stream which then passed a 0.45 $\mu$m Millipore filter on which the crud was collected.

### *2.2 Sample pre-treatment for XRD/ SEM analysis and ICP-AES measurement*

For XRD and SEM measurements, the sample was cut a very small fraction of the whole filter paper. In order to analyze the chemical composition of the crud by wet chemical techniques and gamma spectrometry the complete filter samples were dissolved. All cruds on filters were completely dissolved in mixture of $HNO_3$ (69%) HCl (37%) and $H_2O_2$ (30%) in the Teflon containers and were evaporated to near dryness on the hot plate and then diluted to volumetric flask for quantitative analysis.

*2.3 Scanning Electron Microscope (SEM; JEOL, JSM-6510 )*

The crud samples were placed on the carbon/copper sample stand (area of 10 x 10 mm) with electro-conductible double-sided tape. After drying under infrared lamp (250W) for about 30 minutes, the dried sample was put into the vacuum chamber of sputter-coating machine for vacuuming.

*2.4 X-Ray Diffractometer (XRD; Bruker D8 Advance)*

The instrument was equipped with Cu X-Ray tube. The current and voltage of X-Ray was set to 40 mA and 40 kV, respectively. The computer was used to compare the sample and reference diffraction spectra and then the crystal contents of samples could be determined.

*2.5 Inductively coupled plasma-atomic emission spectroscopy (ICP-AES; Jobin Yvon JY-38S, Japan )*

The average elemental composition (Fe, Co, Cu, Ni, Cr, Zn and Mn) of depositing corrosion products on fuel surface were measured with ICP-AES after sample pretreatment.

*2.6 Gamma spectrometer*

The radioactivity of samples with the crud was measured with high purity Ge-detector (Canberra GC 4020) and a 1024 multi-channel analyzer (Canberra DSP 9660). The activity concentrations of $^{54}$Mn, $^{60}$Co, $^{58}$Co and $^{59}$Fe were calculated from the gamma spectra.

## 3. Results and discussions

*3.1 Chemical analysis of elemental compositions for deposits*

The average concentration of metallic insoluble (CRUD) and soluble species in the reactor water from EOC 19 to EOC 21 was listed in Table 1. The average metallic compositions of corrosion deposits detected by ICP-AES on the fuel surface were also displayed in Table 2. From Table 1 and Table 2, except for Fe, it was found that trace elements including Cu, Ni, Cr and Zn, had a lower deposition on fuel surfaces, although copper nickel condenser tube was used at this plant.

Table1 The average concentration of metallic species in the reactor water

| Average concentration | | Fe | Cu | Ni | Cr | Zn |
|---|---|---|---|---|---|---|
| Insoluble | Concentration (ppb) | 2.57 | 0.31 | 0.21 | 0.21 | 0.45 |
| | Weight composition (wt%) | 68.53 | 8.27 | 5.60 | 5.60 | 12.00 |
| Soluble | Concentration (ppb) | 2.09 | 1.26 | 0.30 | 0.21 | 0.91 |
| | Weight composition (wt%) | 43.82 | 26.42 | 6.29 | 4.40 | 19.08 |

Table 2 Average elemental composition of depositing corrosion products on fuel surface

| Fuel assembly | K1D015 | | K1D059 | | Total average |
|---|---|---|---|---|---|
| Fuel rod / Element | L5 | A5 | L5 | A5 | |
| Fe | 96.97 | 96.80 | 97.22 | 96.91 | 96.98 |
| Co | 0.07 | 0.06 | 0.05 | 0.07 | 0.06 |
| Cu | 1.56 | 1.55 | 1.54 | 1.70 | 1.59 |
| Ni | 0.59 | 0.61 | 0.49 | 0.49 | 0.55 |
| Cr | 0.16 | 0.33 | 0.15 | 0.17 | 0.20 |
| Zn | 0.40 | 0.37 | 0.32 | 0.38 | 0.37 |
| Mn | 0.28 | 0.28 | 0.26 | 0.28 | 0.28 |
| Total | 100 | 100 | 100 | 100 | 100 |

The axial concentration distributions of Fe, $^{54}$Mn activity, Co, $^{60}$Co activity, Ni and $^{58}$Co activity in the fuel deposits along the fuel rod are shown in Fig. 1 through Fig. 3. The distribution pattern of $^{54}$Mn in

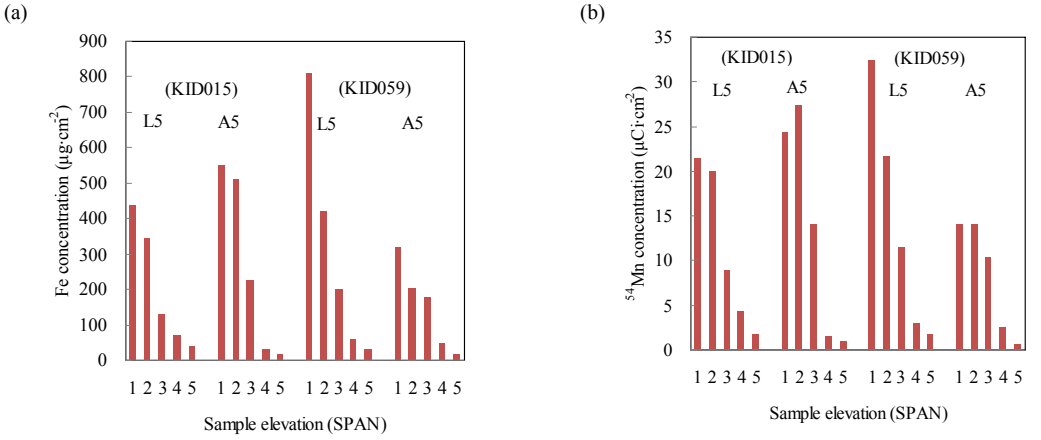


Fig. 1 Deposition profile of (a) Fe concentration and (b) $^{54}$Mn activity concentration at fuel

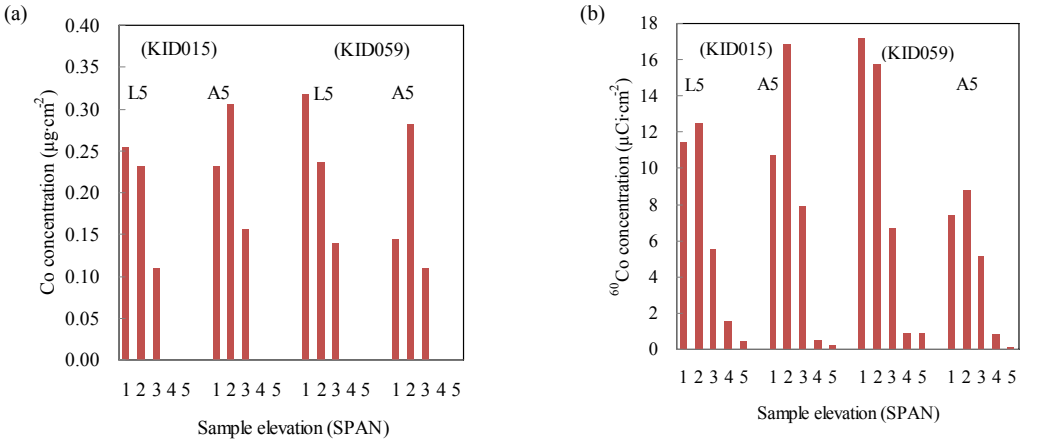


Fig. 2 Deposition profile of (a) Co concentration and (b) $^{60}$Co activity concentration at fuel cycle

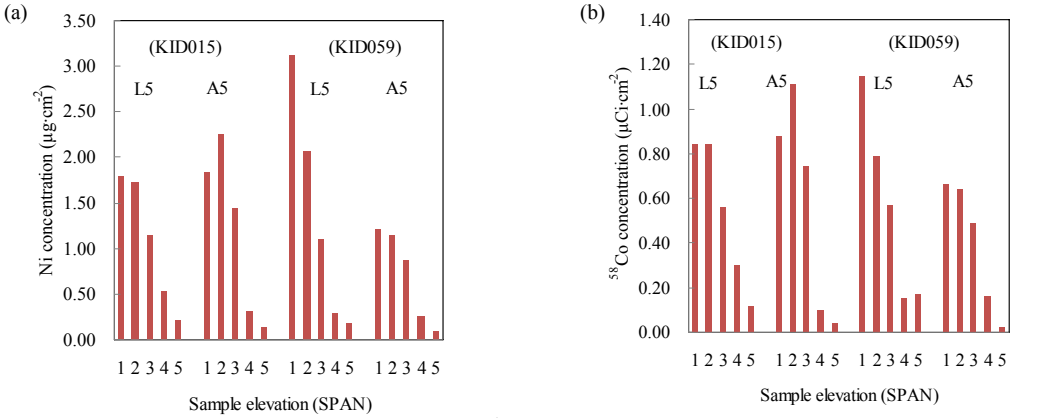


Fig. 3 Deposition profile of (a) Ni concentration and (b) $^{58}$Co activity concentration at fuel cycle

Fig 1 (b) is similar to that of Fig 1 (a), which is reasonable since $^{54}$Fe (natural isotope; 35% abundance) is the mother isotope of $^{54}$Mn via the neutron activation reaction [$^{54}$Fe (n, P) $^{54}$Mn]. The distribution pattern of $^{60}$Co by the neutron irradiation [$^{59}$Co (n, γ) $^{60}$Co] is also similar to Co, however, it has more similarity to that of Fe, as given in Fig 1 (a) and 1 (b). As could be found in Fig. 2 (b) and Fig. 3 (b), $^{60}$Co in some of the plants may be explained by a somewhat higher fraction of reactor water $^{60}$Co than that of $^{58}$Co in the insoluble form. The main reason for this difference is different sources for the nuclides, with $^{60}$Co mainly coming from the fuel crud and $^{58}$Co mainly coming from corrosion of Inconel fuel spacers. Likewise, the axial distributions of $^{58}$Co is also like that of Ni as demonstrated in Fig 3 (a) and 3 (b), because the $^{58}$Co is the daughter isotope of $^{58}$Ni (natural isotope; 68.08% abundance) and activated by the neutron irradiation [$^{58}$Ni (n, P) $^{58}$Co].

*3.2 Scanning Electron Microscope (SEM) morphology*

Fig 4 (a)~(c) show the crud morphology of deposits on the fuel surfaces using SEM. Most of the crud was comprised of the flakes and irregular shapes. A small number of the samples contained visible "flake" crud deposits. Flakes are defined as crud deposit fragments greater than or equal to 5 μm in their largest dimension.

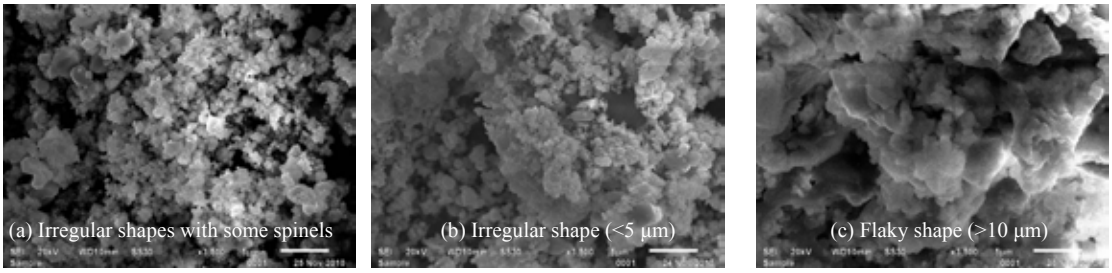


Fig 4. Morphology of CRUD on fuel deposit

*3.3 X-Ray Diffraction (XRD) analysis*

The sample was analyzed by X-ray Diffraction (XRD), suggesting that there was only hematite (α-$Fe_2O_3$) on most of filters. Apparently, there was too little crud present, or the crud was poorly crystallized to produce diffraction lines.

*3.4 Comparison of fuel deposit by calculation and measurement*

The $^{60}$Co transport models of BWR from Uchida et al [7] and Lin et al [8] as well as a model based on the microlayer evaporation and drying out that happened in the nucleate boiling bubble developed by Prof. Uchida [9-10] of Hitachi corp. were adopted and modified to establish the mathematical model of crud deposits. The parameters used in the modified model were based on the design basis and operational data at this unit. It was estimated to be 1.87 mg/cm$^2$ by calculation with the original deposition rate coefficient as used in the model of Uchida et al [7]. The average deposited amounts of crud sample taken from fuel surface at outage of fuel cycle 3 were determined to be approximately 0.24 and 0.23 mg/cm$^2$ for fuel bundles of K1D015 and K1D059, respectively at outage of fuel cycle, which was in agreement with the results of 0.16-0.26 mg/cm$^2$ for normal water chemistry in the previous investigation [6,11]. The difference between the data of modified model prediction and determined value by weighting and measurement is about ten times. If the deposition rate coefficient ($k$), the fraction of iron oxide that deposited on the heated surface was adjusted from 0.3 [12] to 0.03, the consistency will be obtained between the calculated value and analytical result. The value of $k$, 0.03 also indicated that the heated surface deposition of the iron oxide from the vaporized water occurred at a rate of 3% with quite low deposition probability. The modification is comprehensive, because this coefficient in original model of

Uchida et al., was based on saturated depositing crud on BWR fuel surface, i.e., 4-6 mg/cm$^2$, which is approximately higher than one order of calculated value than the measured data in this study

## 4. Conclusions

The off-site analytical results and model prediction from plant data accounted for the effect of reactor water chemistry to the crud compositions on fuel surface of a boiling water reactor when the water chemistry was switched from NWC to HWC and also obtained the following principal conclusions.

1. The studied unit seems to be one BWR plant of lower crud deposition on fuel surface. The deposition rate coefficient of crud in the reactor water on the fuel surface could be estimated to be 1/10-1/8 of the original mathematical model.
2. The major constitute of fuel deposit was hematite ($\alpha$-$Fe_2O_3$), more than 95 wt% via XRD results.
3. Fuel rods exposed to three cycles of HWC showed equivalent to only NWC cycles.

## Acknowledgements

The authors wish to express sincere gratitude to AREVA for the financial supports under contract number FANP-INER S3206. The authors are indebted to Ms. Wan-June Chiu of Institute of Nuclear Energy Research and Mr. Charles F. Chu of Taiwan Power Company for providing technical information and recent plant data, respectively. Dr. Gia-Luen Guo of Bioethanol Project is also gratefully acknowledged for his enthusiastic contributions to the collection of valuable literature and constructive suggestions.

## References

[1] C. C. Lin, F. R. Smith, R. L. Cowan. Effects of hydrogen water chemistry on radiation field buildup in BWRs. *Nucl. Eng. Des.* 166 (1996) 31-36.

[2] C. C. Lin. A review of corrosion product transport and radiation field buildup in boiling water reactors. *Progr. in Nucl. Energy*. 51 (2009) 207-224

[3] J. Kobler Waldis, M. Krois, H.P. Linder, I. Günther-Leopold. *Chemical investigations on CRUD samples*, Progress report 2005-2006 Paul Scherrer Institute (PSI) laboratory for Materials Behavior (LWV).

[4] S. Abolhassani, R. Restani, G. Ledergerber, M. Limbäck. *Recent studies on the examination of crud on high burn-up fuel*, Progress report 2005-2006 Paul Scherrer Institute (PSI) laboratory for Materials Behavior (LWV).

[5] W. J Chiu, S. C Cheng, J. T Lee. *Hydrogen water chemistry fuel surveillance program on Atrium-10 fuel assemblies at Kuosheng unit 1-(KS1-EX5)*, INER-A2401R, Institute of Nuclear Energy Research, Taiwan, R.O.C., Dec., 2010.

[6] S. Uchida, Y. Asakura. Chemical composition of CRUD depositing on BWR fuel surfaces. *J. Nucl. Sci. Technol.* 24 (1987) 385-392.

[7] S. Uchida, M. Kihuchi, Y. Asakura, H. Yusa and K. Ohsumi. A calculation model for predicting concentration of radio corrosion product in the primary coolant of boiling water reactor. *Nucl. Sci. Eng.* 67 (1978) 247-254.

[8] C. C. Lin, C.R. Pao, J.S. Wiley W.R. DeHollander. A mathematical model of corrosion product transport in the boiling water reactor primary system. *Nucl. Technol.* 54 (1981) 253-265

[9]. Y. Asakura, M. Kikuchi, S. Uchida, H. Yusa. Deposition of iron oxide on heated surfaces in boiling water, *Nucl. Sci. Eng.* 67 (1978) 1-7.

[10] Y. Asakura, M. Kikuchi, S. Uchida, H. Yusa. Iron oxide deposition on heated surfaces in pressurized boiling water, *Nucl. Sci. Eng.* 72 (1979) 117-120.

[11] C. H. Liang and C. C Chien. *The effect of reactor water chemistry to the crud compositions on fuel surfaces of one boiling water reactor.* INER-3190H, Institute of Nuclear Energy Research, Taiwan, 2005.

[12] O.H. Charlesworth. Chem. *Eng. Progr. Sym. Ser.*, 2 (1970), p. 21.